FERMILAB-PUB-05-485-E

Search for charged Higgs bosons from top quark decays in $p\bar{p}$ collisions at $\sqrt{s} = 1.96$ TeV

A. Abulencia,[23] D. Acosta,[17] J. Adelman,[13] T. Affolder,[10] T. Akimoto,[53] M.G. Albrow,[16] D. Ambrose,[16]
S. Amerio,[42] D. Amidei,[33] A. Anastassov,[50] K. Anikeev,[16] A. Annovi,[44] J. Antos,[1] M. Aoki,[53] G. Apollinari,[16]
J.-F. Arguin,[32] T. Arisawa,[55] A. Artikov,[14] W. Ashmanskas,[16] A. Attal,[8] F. Azfar,[41] P. Azzi-Bacchetta,[42]
P. Azzurri,[44] N. Bacchetta,[42] H. Bachacou,[28] W. Badgett,[16] A. Barbaro-Galtieri,[28] V.E. Barnes,[46] B.A. Barnett,[24]
S. Baroiant,[7] V. Bartsch,[30] G. Bauer,[31] F. Bedeschi,[44] S. Behari,[24] S. Belforte,[52] G. Bellettini,[44] J. Bellinger,[57]
A. Belloni,[31] E. Ben-Haim,[16] D. Benjamin,[15] A. Beretvas,[16] J. Beringer,[28] T. Berry,[29] A. Bhatti,[48] M. Binkley,[16]
D. Bisello,[42] M. Bishai,[16] R. E. Blair,[2] C. Blocker,[6] K. Bloom,[33] B. Blumenfeld,[24] A. Bocci,[48] A. Bodek,[47]
V. Boisvert,[47] G. Bolla,[46] A. Bolshov,[31] D. Bortoletto,[46] J. Boudreau,[45] S. Bourov,[16] A. Boveia,[10] B. Brau,[10]
C. Bromberg,[34] E. Brubaker,[13] J. Budagov,[14] H.S. Budd,[47] S. Budd,[23] K. Burkett,[16] G. Busetto,[42] P. Bussey,[20]
K. L. Byrum,[2] S. Cabrera,[15] M. Campanelli,[19] M. Campbell,[33] F. Canelli,[8] A. Canepa,[46] D. Carlsmith,[57]
R. Carosi,[44] S. Carron,[15] M. Casarsa,[52] A. Castro,[5] P. Catastini,[44] D. Cauz,[52] M. Cavalli-Sforza,[3] A. Cerri,[28]
L. Cerrito,[41] S.H. Chang,[27] J. Chapman,[33] Y.C. Chen,[1] M. Chertok,[7] G. Chiarelli,[44] G. Chlachidze,[14]
F. Chlebana,[16] I. Cho,[27] K. Cho,[27] D. Chokheli,[14] J.P. Chou,[21] P.H. Chu,[23] S.H. Chuang,[57] K. Chung,[12]
W.H. Chung,[57] Y.S. Chung,[47] M. Ciljak,[44] C.I. Ciobanu,[23] M.A. Ciocci,[44] A. Clark,[19] D. Clark,[6] M. Coca,[15]
A. Connolly,[28] M.E. Convery,[48] J. Conway,[7] B. Cooper,[30] K. Copic,[33] M. Cordelli,[18] G. Cortiana,[42] A. Cruz,[17]
J. Cuevas,[11] R. Culbertson,[16] D. Cyr,[57] S. DaRonco,[42] S. D'Auria,[20] M. D'onofrio,[19] D. Dagenhart,[6]
P. de Barbaro,[47] S. De Cecco,[49] A. Deisher,[28] G. De Lentdecker,[47] M. Dell'Orso,[44] S. Demers,[47] L. Demortier,[48]
J. Deng,[15] M. Deninno,[5] D. De Pedis,[49] P.F. Derwent,[16] C. Dionisi,[49] J.R. Dittmann,[4] P. DiTuro,[50] C. Dörr,[25]
A. Dominguez,[28] S. Donati,[44] M. Donega,[19] P. Dong,[8] J. Donini,[42] T. Dorigo,[42] S. Dube,[50] K. Ebina,[55] J. Efron,[38]
J. Ehlers,[19] R. Erbacher,[7] D. Errede,[23] S. Errede,[23] R. Eusebi,[47] H.C. Fang,[28] S. Farrington,[29] I. Fedorko,[44]
W.T. Fedorko,[13] R.G. Feild,[58] M. Feindt,[25] J.P. Fernandez,[46] R. Field,[17] G. Flanagan,[34] L.R. Flores-Castillo,[45]
A. Foland,[21] S. Forrester,[7] G.W. Foster,[16] M. Franklin,[21] J.C. Freeman,[28] Y. Fujii,[26] I. Furic,[13] A. Gajjar,[29]
M. Gallinaro,[48] J. Galyardt,[12] J.E. Garcia,[44] M. Garcia Sciveres,[28] A.F. Garfinkel,[46] C. Gay,[58] H. Gerberich,[23]
E. Gerchtein,[12] D. Gerdes,[33] S. Giagu,[49] P. Giannetti,[44] A. Gibson,[28] K. Gibson,[12] C. Ginsburg,[16] K. Giolo,[46]
M. Giordani,[52] M. Giunta,[44] G. Giurgiu,[12] V. Glagolev,[14] D. Glenzinski,[16] M. Gold,[36] N. Goldschmidt,[33]
J. Goldstein,[41] G. Gomez,[11] G. Gomez-Ceballos,[11] M. Goncharov,[51] O. González,[46] I. Gorelov,[36] A.T. Goshaw,[15]
Y. Gotra,[45] K. Goulianos,[48] A. Gresele,[42] M. Griffiths,[29] S. Grinstein,[21] C. Grosso-Pilcher,[13] U. Grundler,[23]
J. Guimaraes da Costa,[21] C. Haber,[28] S.R. Hahn,[16] K. Hahn,[43] E. Halkiadakis,[47] A. Hamilton,[32] B.-Y. Han,[47]
R. Handler,[57] F. Happacher,[18] K. Hara,[53] M. Hare,[54] S. Harper,[41] R.F. Harr,[56] R.M. Harris,[16] K. Hatakeyama,[48]
J. Hauser,[8] C. Hays,[15] H. Hayward,[29] A. Heijboer,[43] B. Heinemann,[29] J. Heinrich,[43] M. Hennecke,[25] M. Herndon,[57]
J. Heuser,[25] D. Hidas,[15] C.S. Hill,[10] D. Hirschbuehl,[25] A. Hocker,[16] A. Holloway,[21] S. Hou,[1] M. Houlden,[29]
S.-C. Hsu,[9] B.T. Huffman,[41] R.E. Hughes,[38] J. Huston,[34] K. Ikado,[55] J. Incandela,[10] G. Introzzi,[44] M. Iori,[49]
Y. Ishizawa,[53] A. Ivanov,[7] B. Iyutin,[31] E. James,[16] D. Jang,[50] B. Jayatilaka,[33] D. Jeans,[49] H. Jensen,[16]
E.J. Jeon,[27] M. Jones,[46] K.K. Joo,[27] S.Y. Jun,[12] T.R. Junk,[23] T. Kamon,[51] J. Kang,[33] M. Karagoz-Unel,[37]
P.E. Karchin,[56] Y. Kato,[40] Y. Kemp,[25] R. Kephart,[16] U. Kerzel,[25] V. Khotilovich,[51] B. Kilminster,[38] D.H. Kim,[27]
H.S. Kim,[27] J.E. Kim,[27] M.J. Kim,[12] M.S. Kim,[27] S.B. Kim,[27] S.H. Kim,[53] Y.K. Kim,[13] M. Kirby,[15] L. Kirsch,[6]
S. Klimenko,[17] M. Klute,[31] B. Knuteson,[31] B.R. Ko,[15] H. Kobayashi,[53] K. Kondo,[55] D.J. Kong,[27] J. Konigsberg,[17]
K. Kordas,[18] A. Korytov,[17] A.V. Kotwal,[15] A. Kovalev,[43] J. Kraus,[23] I. Kravchenko,[31] M. Kreps,[25] A. Kreymer,[16]
J. Kroll,[43] N. Krumnack,[4] M. Kruse,[15] V. Krutelyov,[51] S. E. Kuhlmann,[2] Y. Kusakabe,[55] S. Kwang,[13]
A.T. Laasanen,[46] S. Lai,[32] S. Lami,[44] S. Lammel,[16] M. Lancaster,[30] R.L. Lander,[7] K. Lannon,[38] A. Lath,[50]
G. Latino,[44] I. Lazzizzera,[42] C. Lecci,[25] T. LeCompte,[2] J. Lee,[47] J. Lee,[27] S.W. Lee,[51] R. Lefèvre,[3] N. Leonardo,[31]
S. Leone,[44] S. Levy,[13] J.D. Lewis,[16] K. Li,[58] C. Lin,[58] C.S. Lin,[16] M. Lindgren,[16] E. Lipeles,[9] T.M. Liss,[23]
A. Lister,[19] D.O. Litvintsev,[16] T. Liu,[16] Y. Liu,[19] N.S. Lockyer,[43] A. Loginov,[35] M. Loreti,[42] P. Loverre,[49]
R.-S. Lu,[1] D. Lucchesi,[42] P. Lujan,[28] P. Lukens,[16] G. Lungu,[17] L. Lyons,[41] J. Lys,[28] R. Lysak,[1] E. Lytken,[46]
P. Mack,[25] D. MacQueen,[32] R. Madrak,[16] K. Maeshima,[16] P. Maksimovic,[24] G. Manca,[29] F. Margaroli,[5]
R. Marginean,[16] C. Marino,[23] A. Martin,[58] M. Martin,[24] V. Martin,[37] M. Martínez,[3] T. Maruyama,[53]
H. Matsunaga,[53] M.E. Mattson,[56] R. Mazini,[32] P. Mazzanti,[5] K.S. McFarland,[47] D. McGivern,[30] P. McIntyre,[51]
P. McNamara,[50] R. McNulty,[29] A. Mehta,[29] S. Menzemer,[31] A. Menzione,[44] P. Merkel,[46] C. Mesropian,[48]

A. Messina,[49] M. von der Mey,[8] T. Miao,[16] N. Miladinovic,[6] J. Miles,[31] R. Miller,[34] J.S. Miller,[33] C. Mills,[10] M. Milnik,[25] R. Miquel,[28] S. Miscetti,[18] G. Mitselmakher,[17] A. Miyamoto,[26] N. Moggi,[5] B. Mohr,[8] R. Moore,[16] M. Morello,[44] P. Movilla Fernandez,[28] J. Mülmenstädt,[28] A. Mukherjee,[16] M. Mulhearn,[31] Th. Muller,[25] R. Mumford,[24] P. Murat,[16] J. Nachtman,[16] S. Nahn,[58] I. Nakano,[39] A. Napier,[54] D. Naumov,[36] V. Necula,[17] C. Neu,[43] M.S. Neubauer,[9] J. Nielsen,[28] T. Nigmanov,[45] L. Nodulman,[2] O. Norniella,[3] T. Ogawa,[55] S.H. Oh,[15] Y.D. Oh,[27] T. Okusawa,[40] R. Oldeman,[29] R. Orava,[22] K. Osterberg,[22] C. Pagliarone,[44] E. Palencia,[11] R. Paoletti,[44] V. Papadimitriou,[16] A. Papikonomou,[25] A.A. Paramonov,[13] B. Parks,[38] S. Pashapour,[32] J. Patrick,[16] G. Pauletta,[52] M. Paulini,[12] C. Paus,[31] D.E. Pellett,[7] A. Penzo,[52] T.J. Phillips,[15] G. Piacentino,[44] J. Piedra,[11] K. Pitts,[23] C. Plager,[8] L. Pondrom,[57] G. Pope,[45] X. Portell,[3] O. Poukhov,[14] N. Pounder,[41] F. Prakoshyn,[14] A. Pronko,[16] J. Proudfoot,[2] F. Ptohos,[18] G. Punzi,[44] J. Pursley,[24] J. Rademacker,[41] A. Rahaman,[45] A. Rakitin,[31] S. Rappoccio,[21] F. Ratnikov,[50] B. Reisert,[16] V. Rekovic,[36] N. van Remortel,[22] P. Renton,[41] M. Rescigno,[49] S. Richter,[25] F. Rimondi,[5] K. Rinnert,[25] L. Ristori,[44] W.J. Robertson,[15] A. Robson,[20] T. Rodrigo,[11] E. Rogers,[23] S. Rolli,[54] R. Roser,[16] M. Rossi,[52] R. Rossin,[17] C. Rott,[46] A. Ruiz,[11] J. Russ,[12] V. Rusu,[13] D. Ryan,[54] H. Saarikko,[22] S. Sabik,[32] A. Safonov,[7] W.K. Sakumoto,[47] G. Salamanna,[49] O. Salto,[3] D. Saltzberg,[8] C. Sanchez,[3] L. Santi,[52] S. Sarkar,[49] K. Sato,[53] P. Savard,[32] A. Savoy-Navarro,[16] T. Scheidle,[25] P. Schlabach,[16] E.E. Schmidt,[16] M.P. Schmidt,[58] M. Schmitt,[37] T. Schwarz,[33] L. Scodellaro,[11] A.L. Scott,[10] A. Scribano,[44] F. Scuri,[44] A. Sedov,[46] S. Seidel,[36] Y. Seiya,[40] A. Semenov,[14] F. Semeria,[5] L. Sexton-Kennedy,[16] I. Sfiligoi,[18] M.D. Shapiro,[28] T. Shears,[29] P.F. Shepard,[45] D. Sherman,[21] M. Shimojima,[53] M. Shochet,[13] Y. Shon,[57] I. Shreyber,[35] A. Sidoti,[44] A. Sill,[16] P. Sinervo,[32] A. Sisakyan,[14] J. Sjolin,[41] A. Skiba,[25] A.J. Slaughter,[16] K. Sliwa,[54] D. Smirnov,[36] J. R. Smith,[7] F.D. Snider,[16] R. Snihur,[32] M. Soderberg,[33] A. Soha,[7] S. Somalwar,[50] V. Sorin,[34] J. Spalding,[16] F. Spinella,[44] P. Squillacioti,[44] M. Stanitzki,[58] A. Staveris-Polykalas,[44] R. St. Denis,[20] B. Stelzer,[8] O. Stelzer-Chilton,[32] D. Stentz,[37] J. Strologas,[36] D. Stuart,[10] J.S. Suh,[27] A. Sukhanov,[17] K. Sumorok,[31] H. Sun,[54] T. Suzuki,[53] A. Taffard,[23] R. Tafirout,[32] R. Takashima,[39] Y. Takeuchi,[53] K. Takikawa,[53] M. Tanaka,[2] R. Tanaka,[39] M. Tecchio,[33] P.K. Teng,[1] K. Terashi,[48] S. Tether,[31] J. Thom,[16] A.S. Thompson,[20] E. Thomson,[43] P. Tipton,[47] V. Tiwari,[12] S. Tkaczyk,[16] D. Toback,[51] K. Tollefson,[34] T. Tomura,[53] D. Tonelli,[44] M. Tönnesmann,[34] S. Torre,[44] D. Torretta,[16] S. Tourneur,[16] W. Trischuk,[32] R. Tsuchiya,[55] S. Tsuno,[39] N. Turini,[44] F. Ukegawa,[53] T. Unverhau,[20] S. Uozumi,[53] D. Usynin,[43] L. Vacavant,[28] A. Vaiciulis,[47] S. Vallecorsa,[19] A. Varganov,[33] E. Vataga,[36] G. Velev,[16] G. Veramendi,[23] V. Veszpremi,[46] T. Vickey,[23] R. Vidal,[16] I. Vila,[11] R. Vilar,[11] I. Vollrath,[32] I. Volobouev,[28] F. Würthwein,[9] P. Wagner,[51] R. G. Wagner,[2] R.L. Wagner,[16] W. Wagner,[25] R. Wallny,[8] T. Walter,[25] Z. Wan,[50] M.J. Wang,[1] S.M. Wang,[17] A. Warburton,[32] B. Ward,[20] S. Waschke,[20] D. Waters,[30] T. Watts,[50] M. Weber,[28] W.C. Wester III,[16] B. Whitehouse,[54] D. Whiteson,[43] A.B. Wicklund,[2] E. Wicklund,[16] H.H. Williams,[43] P. Wilson,[16] B.L. Winer,[38] P. Wittich,[43] S. Wolbers,[16] C. Wolfe,[13] S. Worm,[50] T. Wright,[33] X. Wu,[19] S.M. Wynne,[29] A. Yagil,[16] K. Yamamoto,[40] J. Yamaoka,[50] Y. Yamashita.,[39] C. Yang,[58] U.K. Yang,[13] W.M. Yao,[28] G.P. Yeh,[16] J. Yoh,[16] K. Yorita,[13] T. Yoshida,[40] I. Yu,[27] S.S. Yu,[43] J.C. Yun,[16] L. Zanello,[49] A. Zanetti,[52] I. Zaw,[21] F. Zetti,[44] X. Zhang,[23] J. Zhou,[50] and S. Zucchelli[5]

(CDF Collaboration)

[1]*Institute of Physics, Academia Sinica, Taipei, Taiwan 11529, Republic of China*
[2]*Argonne National Laboratory, Argonne, Illinois 60439*
[3]*Institut de Fisica d'Altes Energies, Universitat Autonoma de Barcelona, E-08193, Bellaterra (Barcelona), Spain*
[4]*Baylor University, Waco, Texas 76798*
[5]*Istituto Nazionale di Fisica Nucleare, University of Bologna, I-40127 Bologna, Italy*
[6]*Brandeis University, Waltham, Massachusetts 02254*
[7]*University of California, Davis, Davis, California 95616*
[8]*University of California, Los Angeles, Los Angeles, California 90024*
[9]*University of California, San Diego, La Jolla, California 92093*
[10]*University of California, Santa Barbara, Santa Barbara, California 93106*
[11]*Instituto de Fisica de Cantabria, CSIC-University of Cantabria, 39005 Santander, Spain*
[12]*Carnegie Mellon University, Pittsburgh, PA 15213*
[13]*Enrico Fermi Institute, University of Chicago, Chicago, Illinois 60637*
[14]*Joint Institute for Nuclear Research, RU-141980 Dubna, Russia*
[15]*Duke University, Durham, North Carolina 27708*
[16]*Fermi National Accelerator Laboratory, Batavia, Illinois 60510*
[17]*University of Florida, Gainesville, Florida 32611*
[18]*Laboratori Nazionali di Frascati, Istituto Nazionale di Fisica Nucleare, I-00044 Frascati, Italy*
[19]*University of Geneva, CH-1211 Geneva 4, Switzerland*

[20]*Glasgow University, Glasgow G12 8QQ, United Kingdom*
[21]*Harvard University, Cambridge, Massachusetts 02138*
[22]*Division of High Energy Physics, Department of Physics,*
University of Helsinki and Helsinki Institute of Physics, FIN-00014, Helsinki, Finland
[23]*University of Illinois, Urbana, Illinois 61801*
[24]*The Johns Hopkins University, Baltimore, Maryland 21218*
[25]*Institut für Experimentelle Kernphysik, Universität Karlsruhe, 76128 Karlsruhe, Germany*
[26]*High Energy Accelerator Research Organization (KEK), Tsukuba, Ibaraki 305, Japan*
[27]*Center for High Energy Physics: Kyungpook National University, Taegu 702-701; Seoul National University,*
Seoul 151-742; and SungKyunKwan University, Suwon 440-746; Korea
[28]*Ernest Orlando Lawrence Berkeley National Laboratory, Berkeley, California 94720*
[29]*University of Liverpool, Liverpool L69 7ZE, United Kingdom*
[30]*University College London, London WC1E 6BT, United Kingdom*
[31]*Massachusetts Institute of Technology, Cambridge, Massachusetts 02139*
[32]*Institute of Particle Physics: McGill University, Montréal,*
Canada H3A 2T8; and University of Toronto, Toronto, Canada M5S 1A7
[33]*University of Michigan, Ann Arbor, Michigan 48109*
[34]*Michigan State University, East Lansing, Michigan 48824*
[35]*Institution for Theoretical and Experimental Physics, ITEP, Moscow 117259, Russia*
[36]*University of New Mexico, Albuquerque, New Mexico 87131*
[37]*Northwestern University, Evanston, Illinois 60208*
[38]*The Ohio State University, Columbus, Ohio 43210*
[39]*Okayama University, Okayama 700-8530, Japan*
[40]*Osaka City University, Osaka 588, Japan*
[41]*University of Oxford, Oxford OX1 3RH, United Kingdom*
[42]*University of Padova, Istituto Nazionale di Fisica Nucleare,*
Sezione di Padova-Trento, I-35131 Padova, Italy
[43]*University of Pennsylvania, Philadelphia, Pennsylvania 19104*
[44]*Istituto Nazionale di Fisica Nucleare Pisa, Universities of Pisa,*
Siena and Scuola Normale Superiore, I-56127 Pisa, Italy
[45]*University of Pittsburgh, Pittsburgh, Pennsylvania 15260*
[46]*Purdue University, West Lafayette, Indiana 47907*
[47]*University of Rochester, Rochester, New York 14627*
[48]*The Rockefeller University, New York, New York 10021*
[49]*Istituto Nazionale di Fisica Nucleare, Sezione di Roma 1,*
University of Rome "La Sapienza," I-00185 Roma, Italy
[50]*Rutgers University, Piscataway, New Jersey 08855*
[51]*Texas A&M University, College Station, Texas 77843*
[52]*Istituto Nazionale di Fisica Nucleare, University of Trieste/ Udine, Italy*
[53]*University of Tsukuba, Tsukuba, Ibaraki 305, Japan*
[54]*Tufts University, Medford, Massachusetts 02155*
[55]*Waseda University, Tokyo 169, Japan*
[56]*Wayne State University, Detroit, Michigan 48201*
[57]*University of Wisconsin, Madison, Wisconsin 53706*
[58]*Yale University, New Haven, Connecticut 06520*

(Dated: October 20, 2005)

We report the results of a search for a charged Higgs boson in the decays of top quarks produced in $p\bar{p}$ collisions at a center-of-mass energy of 1.96 TeV. We use a data sample corresponding to an integrated luminosity of 193 pb^{-1} collected by the upgraded Collider Detector at Fermilab. No evidence for charged Higgs production is found, allowing 95% C.L. upper limits to be placed on $\mathrm{BR}(t \to H^+ b)$ for different charged Higgs decay scenarios. In addition, we present in the MSSM ($m_{H^\pm}$,$\tan\beta$) plane the first exclusion regions with radiative and Yukawa coupling corrections.

PACS numbers: 14.65.Ha, 14.80.Cp, 13.85.Qk

One of the open questions in the standard model (SM) of particle physics involves the mechanism of electroweak symmetry breaking (EWSB). Within the SM it is postulated that a single scalar doublet field breaks the symmetry, resulting in a single observable particle of unknown mass called the Higgs boson [1]. To date, the SM Higgs boson has not been observed, and extensions of the SM have been proposed with different Higgs phenomenologies. The simplest extension of the SM Higgs sector is built by the introduction of another Higgs doublet resulting in a two-Higgs doublet model [2]. In these models EWSB results in five Higgs bosons, three of which are neutral (h^0, H^0, A^0) and two of which are charged ($H^\pm$). The minimal supersymmetric extension of the SM

(MSSM) includes a two-Higgs doublet sector in which one doublet couples to the up-type quarks and neutrinos, and the other to the down-type quarks and charged leptons [3]. The observation of a charged Higgs boson would provide unambiguous evidence of a Higgs sector richer than that predicted by the SM.

At the Tevatron, direct production of H^+H^- via the weak interaction is expected to have a relatively small cross section on the order of 0.1 pb [4]. The production of $t\bar{t}$ pairs, with a theoretical production cross section of $6.7^{+0.7}_{-0.9}$ pb [5, 6] for m_t =175 GeV/c^2, may offer another source of charged Higgs production. If kinematically allowed, the top quark can decay to H^+b, competing with the SM decay $t \to W^+b$. This mechanism can provide a larger production rate of charged Higgs and offers a much cleaner signature than that of direct production.

Previous searches for the charged Higgs boson have been performed at $\sqrt{s} = 1.8$ TeV in the $\tau_h + \not\!\!E_T + \text{jets} + \ell$ channels, where $\not\!\!E_T$ is defined in [7], τ_h denotes a tau lepton which decays to hadrons, and where $\ell = e$ or μ in [8] and $\ell = e, \mu$ or τ_h in [9]. In the framework of the tauonic Higgs model, in which the charged Higgs decays exclusively to $\bar{\tau}\nu$, these searches set limits directly on BR($t \to H^+b$) based on the measured production rate. These results are then translated into limits on $\tan\beta$, the ratio of vacuum expectation values of the two Higgs doublets.

Another search for charged Higgs bosons in the $\not\!\!E_T$ + jets + ℓ channel, where $\ell = e$ or μ [10], obtains limits in the ($m_{H^\pm}$,$\tan\beta$) plane assuming that the charged Higgs decays to $\bar{\tau}\nu$, $c\bar{s}$, and $t^*\bar{b}$ ($\to W^+b\bar{b}$). These limits utilize tree-level MSSM predictions of the $t \to H^+b$ and charged Higgs branching fraction as a function of $\tan\beta$. It is now known that higher-order radiative corrections significantly modify these predictions. The corrections strongly depend on the parameters of the model and are particularly large at high values of $\tan\beta$ [11]. In addition, it is also predicted that in the low $\tan\beta$ region, the charged Higgs has a sizable branching fraction to W^+h^0, invalidating the assumption that the charged Higgs decays only to $\bar{\tau}\nu$, $c\bar{s}$ or $t^*\bar{b}$.

CDF has recently reported measurements of the $t\bar{t}$ production cross section in the $\ell + \not\!\!E_T$ + jets + X channels, where $\ell = e, \mu$ and where $X = \ell$ (the "dilepton" channel), $X = \tau_h$ ("lepton+tau"), X = one or more tagged jets [12] ("lepton+jets, ≥ 1 tag"), and X = two or more tagged jets ("lepton+jets, ≥ 2 tags"). These measurements are carried out under the assumption BR($t \to H^+b$) = 0 and use data samples corresponding to an integrated luminosity of up to 193 pb^{-1} [13–15]. Each measurement agrees with the SM $t\bar{t}$ cross section expectation within its uncertainty, providing no evidence for non-SM physics. In this analysis, we consider the possibility of $t \to H^+b$ and recast the cross section results to set limits on charged Higgs production. Depending on the top and Higgs branching ratios, the number of expected events in these decay channels can show an excess or deficit with respect to SM expectations.

TABLE I: Number of events in each exclusive channel from background sources, observed in data, and expected for $\sigma_{t\bar{t}}^{\text{prod}} = 6.7$ pb assuming $BR(t \to H^+b) = 0$.

Channel	Background events	Data events	SM-expected events
dilepton	2.7 ± 0.7	13	10.9 ± 1.4
lepton+jets, = 1 tag	21.8 ± 3.0	49	54.0 ± 4.3
lepton+jets, ≥ 2 tags	1.3 ± 0.3	8	10 ± 1
lepton + tau	1.3 ± 0.2	2	2.3 ± 0.3

As published, these measurements allow the categorization of a single event in multiple channels. In this analysis extra requirements are applied to each channel in order to force the association of every event to a single channel. The acceptance and background contribution to each of these exclusive channels are recalculated, and the changes from the original cross section analyses are found to be mostly negligible. The only exception to this is the "≥ 1 tag" and "≥ 2 tags" lepton+jets channels, where the latter is a proper subset of the former. Removal of this 100% overlap changes the "≥ 1 tag" channel to exactly one tag,"= 1 tag". The results for these new exclusive channels, in terms of background, number of observed events and number of SM expected events are shown in Table I.

We assume that the charged Higgs boson can decay only to $\bar{\tau}\nu$, $c\bar{s}$, $t^*\bar{b}$ or W^+h^0, leading to five possible decay modes for a single top quark: (1) $t \to W^+b$, (2) $t \to H^+b$, $H^+ \to \bar{\tau}\nu$, (3) $t \to H^+b$, $H^+ \to c\bar{s}$, (4) $t \to H^+b$, $H^+ \to t^*\bar{b}$, and (5) $t \to H^+b$, $H^+ \to W^+h^0$, $\text{h}^0 \to \text{b}\bar{\text{b}}$. Charge conjugated decays are implied.

Allowing for a non-zero BR($t \to H^+b$), the acceptance of the detector for channel k is

$$\mathcal{A}_k = \sum_{i,j=1}^{5} B_i \cdot B_j \cdot \epsilon_{ij,k}(\Gamma_t, \Gamma_{H^\pm}, m_{H^\pm}, m_{h^0}), \qquad (1)$$

where B_i (B_j) represent the branching fractions of the top quark (anti-quark) to decay via mode i (j) as listed above, and $\epsilon_{ij,k}$ is the efficiency to detect a $t\bar{t}$ event whose top quarks decay via modes i and j in channel k.

The branching ratios B_2 to B_5 can be factorized as $B_i = \text{BR}(t \to H^+b) \times \text{BR}(H^+ \to X_i)$, where X_i represent the decay products of the charged Higgs. Thus, the five branching ratios B_i can be written in terms of BR($t \to H^+b$), BR($H^+ \to c\bar{s}$), BR($H^+ \to t^*\bar{b}$), BR($H^+ \to W^+h^0$), and BR($h^0 \to b\bar{b}$), where we have used the additional assumed constraint that the branching fraction of the charged Higgs summed over its four possible decay modes adds up to unity.

The efficiencies $\epsilon_{ij,k}$ are obtained from Monte Carlo (MC) simulation of $t\bar{t}$ events generated with different masses of the top, $H^{\pm}$, and h^0. The MC generator PYTHIA [16] is modified to include the decay $H^+ \to t^*\bar{b}$ and is used for the generation of the $t\bar{t}$ events.

The detector simulation and reconstruction algorithms for muons, electrons, and jets are identical to those used in the SM $t\bar{t}$ cross section measurements for the four channels. MC efficiencies are scaled for known differences between MC simulation of the detector response and that observed in data. The dependence of the efficiencies on the width of the top quark (Γ_t) and the width of the charged Higgs ($\Gamma_{H^{\pm}}$) is taken into account using the simulated $t\bar{t}$ events. The systematic uncertainties on $\epsilon_{ij,k}$ for the process $t\bar{t} \to W^+bW^-\bar{b}$ are listed in [13–15] and do not differ much for the other possible decay modes.

The expected number of events in channel k is

$$\mu_k = \sigma_{t\bar{t}}^{\text{prod}} \cdot \mathcal{A}_k(\rho) \cdot \mathcal{L}_k + n_k^{\text{back}}, \tag{2}$$

where $\sigma_{t\bar{t}}^{\text{prod}}$ is the $t\bar{t}$ production cross section and ρ represents a generic model from which the nine quantities (five BR's, Γ_t, $\Gamma_{H^{\pm}}$, $m_{H^{\pm}}$ and m_{h^0}), needed to calculate the acceptance $\mathcal{A}_k$, can be derived. $\mathcal{L}_k$ is the integrated luminosity, and n_k^{back} is the number of expected background events in channel k (shown in Table I). We assume the inclusion of the Higgs sector does not modify the value of the $t\bar{t}$ production cross section and set it to $\sigma_{t\bar{t}}^{\text{prod}} = 6.7 \pm 0.9$ pb.

For each channel a likelihood is constructed based on the Poisson probability to observe N_k events when a given model predicts μ_k events. Since the four channels were constructed to be mutually exclusive, the product of their likelihoods is taken to form a final likelihood. The correlations of the efficiencies, backgrounds, and systematic uncertainties between channels are taken into account. The posterior probability distribution of the parameter of interest is constructed from the likelihood and a prior probability density. The posterior probability is integrated to determine the excluded values of the parameter.

In the MSSM the nine quantities needed to calculate the acceptance are predicted from a specific set of MSSM parameters, including $m_{H^{\pm}}$ and $\tan\beta$. We use the computational package CPsuperH [17] to compute all the Higgs masses and branching ratios. This program includes QCD, SUSY-QCD, and SUSY-EW radiative corrections up to the two-loop leading logarithms and applies these corrections to the top and bottom Yukawa couplings. The top branching ratio to charged Higgs is computed with the same level of accuracy from custom code developed in collaboration with the authors of [11]. In the context of the MSSM with $m_{A^0} < m_{H^{\pm}}$, CPsuperH predicts that the H^+ decay to W^+A^0 is non-negligible for masses of $H^{\pm}$ below 100 GeV/c^2. In this case CPsuperH also predicts the mass of the A^0 to be similar to that of the h^0, and we assume the kinematics of the decay to W^+A^0 to be identical to that of W^+h^0 when the h^0 and A^0 masses are equal. Thus, we assign to the decay $H^+ \to W^+h^0$ a branching ratio of BR($H^+ \to W^+h^0$) + BR($H^+ \to W^+A^0$), effectively considering both decays.

As an example of how a charged Higgs alters the balance between the top decay channels, Fig. 1(a) shows the expected number of events in each of the exclusive channels as a function of $\tan\beta$ for $m_{H^{\pm}} = 120$ GeV/c^2. The other relevant MSSM parameters are detailed in the caption. The figure demonstrates the excess expected in the lepton+tau channel and the deficit expected in the other channels for large $\tan\beta$ values. For values of $\tan\beta$ around 7 the BR($t \to H^+b$) goes to zero and the SM expectation for the different channels is recovered. The relationship between the channels changes with charged Higgs mass. For higher charged Higgs masses the decay $H^+ \to t^*\bar{b}$ is enhanced at low values of $\tan\beta$, leading in this region to an excess of lepton+jets events with two or more tags and a more pronounced deficit of lepton+jets events with exactly one tag. Values of $\tan\beta$ in which CPsuperH reports inconsistencies in the calculation of the Higgs sector are considered theoretically inaccessible.

Figure 1(b) shows the posterior probability obtained for the four channels when the number of SM-expected events is used instead of the number of observed events. The posterior is obtained by means of a flat prior in $\log_{10}(\tan\beta)$. This prior allows for a smooth variation of the top and charged Higgs branching ratios as a function of $\log_{10}(\tan\beta)$. The probability is integrated over its maximum density region to obtain upper and lower limits in $\tan\beta$ at the 95% confidence level (C.L.)

Using the number of events observed in the data and repeating this procedure for different Higgs masses results in the exclusion region shown in Fig. 2. We determine this exclusion region for several sets of benchmark parameters, including the maximal and minimal light Higgs mass scenarios described in [19]. The complete characterization of these scenarios and their results are described in [20]. In all the benchmarks used, the low $\tan\beta$ region is excluded in a similar region as shown in Fig. 2. The high $\tan\beta$ exclusion region, however, can be significantly reduced and even vanishes, due to parameters of particular benchmarks that suppress BR($t \to H^+b$). The obtained exclusion limits strongly depend on the prior probability used. Using a flat prior in $\tan\beta$, which is characterized by sudden changes in the top and charged Higgs branching ratios, yields significantly different exclusion regions. It is important to note that even if all the corrections were turned off, and tree-level calculations were used, the results would be significantly stonger than those obtained in [10] under the same conditions.

In the high $\tan\beta$ region the decay $H^+ \to \bar{\tau}\nu$ is expected to dominate in a large fraction of the MSSM parameter space. In this region the tauonic Higgs model is a

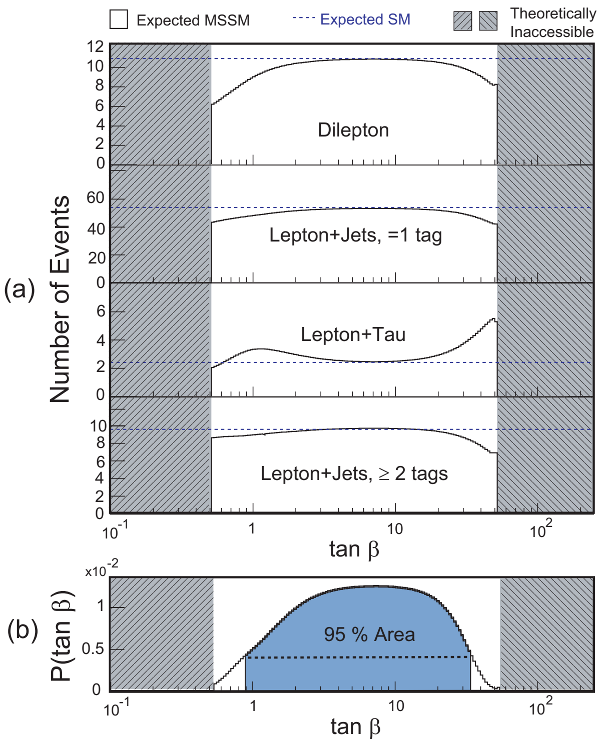

FIG. 1: Predictions for $m_{H^\pm} = 120$ GeV/c^2 and $m_t = 175$ GeV/c^2 as a function of $\tan\beta$ for 193 pb^{-1}. The MSSM parameters are defined in [2] and are set to $M_{SUSY} = 1000$ GeV/c^2, $\mu = -500$ GeV/c^2, $A_t = A_b = 2000$ GeV/c^2, $A_\tau = 500$ GeV/c^2, $M_2 = M_3 = M_Q = M_U = M_D = M_E = M_L = M_{SUSY}$, and $M_1 = 0.498 M_2$. The regions $\tan\beta < 0.505$ and $\tan\beta > 51$ are considered theoretically inaccessible. (a) Expected number of events in each of the channels. (b) Posterior probability density obtained when the number of SM-expected events is used instead of the number of observed events. A flat prior in $\log_{10}(\tan\beta)$ is used.

good approximation, and we explicitly set BR($H^+ \to \bar{\tau}\nu$) = 1 and evaluate the posterior probability as a function of BR($t \to H^+ b$). The value of $\Gamma_{H^\pm}$ has little effect on the results as width corrections to the efficiency are small; we set $\Gamma_{H^\pm} = \Gamma_t^{\rm SM} = 1.4$ GeV/c^2. The width of the top is set to $\Gamma_t = \frac{\Gamma_t^{\rm SM}}{1-{\rm BR}(t\to H^+ b)}$, and the values of m_{h^0} and BR($H^+ \to W^+ h^0$) are irrelevant in this model. We perform the scan in BR($t \to H^+ b$) from 0 to 1. A posterior probability density of BR($t \to H^+ b$) is obtained using a flat prior that is constant between 0 and 1 and null elsewhere. The 95% C.L. is obtained by integrating the posterior over the maximum density region. This procedure is repeated for different charged Higgs masses and the 95% C.L. excluded region is shown in Fig. 3 as a function of $m_{H^\pm}$. For $BR(t \to H^+ b) > 0.9$ the width of the top is larger than 14 GeV/c^2 and the analytical corrections to the efficiencies start losing accuracy.

Finally, in order to reduce the model dependence, we place limits on BR($t \to H^+ b$) that hold for any combination of charged Higgs branching ratios. For a specific charged Higgs mass we divide each charged Higgs branching ratio into 21 bins. This results in 1771 possible combinations subject to the relation $\sum_i {\rm BR}(H^+ \to X_i) = 1$. For each combination, we obtain a limit on BR($t \to H^+ b$) assuming BR($h^0 \to b\bar{b}$) = 0.9 and $m_{h^0} = 70$ GeV/c^2. The least restrictive limit is quoted and the analysis is repeated for different charged Higgs masses. The results are shown in Fig. 4.

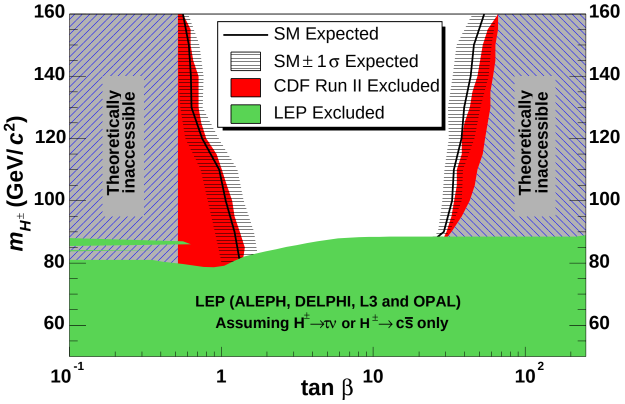

FIG. 2: The MSSM results obtained with 193 pb^{-1} at CDF. The SM-expected exclusion limits are indicated by black solid lines and the $\pm 1\sigma$ confidence band around it is obtained by generating pseudo-experiments. The darkest solid region represents the area excluded at 95% C.L. The solid lower region is the LEP combined results from direct searches [18]. The theoretically inaccessible regions are determined by CPsuperH as explained in the text. Other relevant MSSM parameters are detailed in the caption of Fig. 1.

In summary, we have performed a search for a charged Higgs boson in top quark decays using measurements of the top pair production cross section in four different final states and we find no evidence of signal in the region 80 GeV/c^2 $\leq m_{H^\pm} \leq$ 160 GeV/c^2. In the context of the MSSM with full radiative corrections we exclude the low $\tan\beta$ region for all benchmarks in [20]. The high $\tan\beta$ region cannot be excluded independent of the MSSM parameters. In the tauonic Higgs model, in which the charged Higgs decays exclusively to $\bar{\tau}\nu$, the BR($t \to H^+ b$) is constrained to be less than 0.4 at 95% C.L. If no assumption is made on the charged Higgs decay, the BR($t \to H^+ b$) is constrained to be less than 0.91 at 95% C.L.

We thank the Fermilab staff and the technical staffs of the participating institutions for their vital contributions. This work was supported by the U.S. Department of Energy and National Science Foundation; the Italian Istituto Nazionale di Fisica Nucleare; the Ministry of Education, Culture, Sports, Science and Technology of Japan; the Natural Sciences and Engineering Research Council of Canada; the National Science Council of the Republic of China; the Swiss National Science Founda-

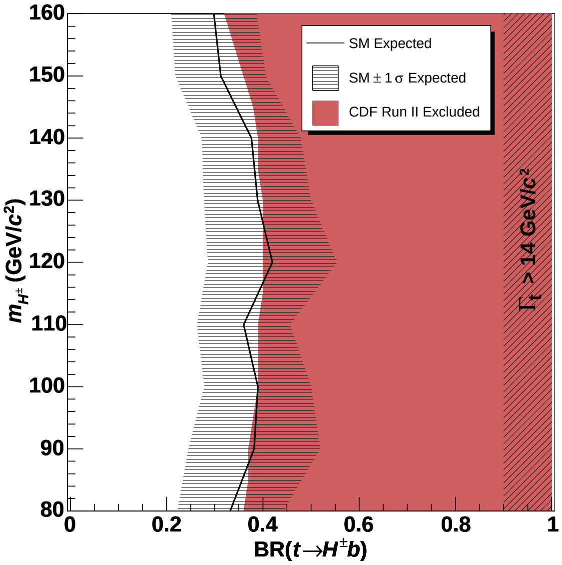

FIG. 3: Results for the tauonic Higgs model with $m_t = 175$ GeV/c^2. The dark solid region represents the CDF Run II excluded region in the ($m_{H^\pm}$,BR($t \rightarrow H^+b$)) plane, assuming BR($H^+ \rightarrow \bar{\tau}\nu$) = 1. The expected exclusion limits are indicated by a black solid line and the $\pm 1\sigma$ confidence band around it is obtained by generating pseudo-experiments. The hatched region of $BR(t \rightarrow H^+b) > 0.9$ indicates that the width of the top is larger than 14 GeV/c^2 .

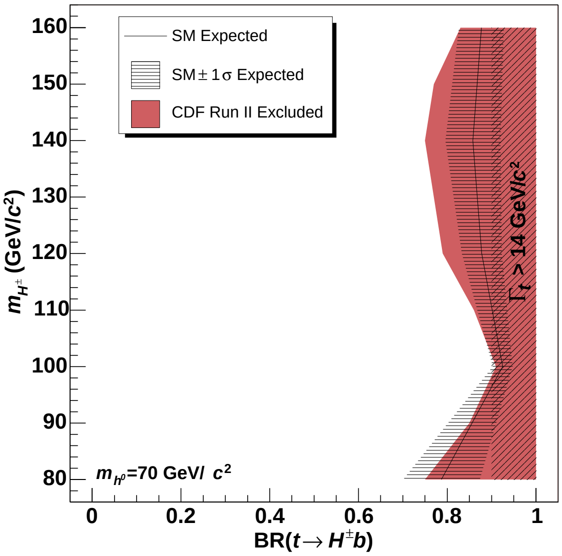

FIG. 4: Results for the charged Higgs branching ratio independent analysis with $m_t = 175$ GeV/c^2. The dark solid region represents the CDF Run II excluded region in the ($m_{H^\pm}$,BR($t \rightarrow H^+b$)) plane. The expected exclusion limits are indicated by a black solid line and the $\pm 1\sigma$ confidence band around it is obtained by generating pseudo-experiments. The hatched region of $BR(t \rightarrow H^+b) > 0.9$ indicates that the width of the top is larger than 14 GeV/c^2.

tion; the A.P. Sloan Foundation; the Bundesministerium für Bildung und Forschung, Germany; the Korean Science and Engineering Foundation and the Korean Research Foundation; the Particle Physics and Astronomy Research Council and the Royal Society, UK; the Russian Foundation for Basic Research; the Comisión Interministerial de Ciencia y Tecnología, Spain; in part by the European Community's Human Potential Programme under contract HPRN-CT-2002-00292; and the Academy of Finland.

---

[1] P. W. Higgs, Phys. Lett. **12**, 132 (1964).
[2] For an introduction, see J. F. Gunion, H. Haber, G. Kane, and S. Dawson, *The Higgs Hunter's Guide*, Frontiers in Physics (Addison-Wesley, Redwood City, CA, 1989).
[3] H. P. Nilles, Phys. Rept. **110**, 1 (1984).
[4] M. Carena and H. E. Haber, Prog. Part. Nucl. Phys. **50**, 63 (2003), hep-ph/0208209.
[5] N. Kidonakis and R. Vogt, Phys. Rev. **D68**, 114014 (2003), hep-ph/0308222.
[6] M. Cacciari, S. Frixione, M. L. Mangano, P. Nason, and G. Ridolfi, J. High Energy Phys. **0404**, 068 (2004), hep-ph/0303085.
[7] We use a cylindrical coordinate system about the beam axis in which θ is the polar angle. We define transverse momentum $p_T = p \sin\theta$ and transverse energy E_T similarly. Missing transverse energy ($\vec{\not{E}}_T$) is defined as $-\sum_i E^i_T \hat{n}_i$, where $\hat{n}_i$ is the unit vector in the azimuthal plane that points from the $p\bar{p}$ interaction region to the i^{th} calorimeter tower. $\vec{\not{E}}_T$ is further corrected for the energy and momentum of identified muons.
[8] T. Affolder et al. (CDF Collaboration), Phys. Rev. D. **62**, 012004 (2000).
[9] F. Abe et al. (CDF Collaboration), Phys. Rev. Lett. **79**, 357 (1997).
[10] B. Abbott et al. (D0 Collaboration), Phys. Rev. Lett. **82**, 4975 (1999).
[11] M. Carena, D. Garcia, U. Nierste, and C. E. M. Wagner, Nucl. Phys. **B577**, 88 (2000), hep-ph/9912516.
[12] A jet is determined to be tagged if it shows a displaced secondary vertex. These jets typically originate from the decay of long lived mesons such as those resulting after the hadronization process of the b quark.
[13] D. Acosta et al. (CDF Collaboration), Phys. Rev. Lett. **93**, 142001 (2004).
[14] S. Demers, Ph.D. thesis, University of Rochester (2005).
[15] D. Acosta et al. (CDF Collaboration), Phys. Rev. **D71**, 052003 (2005), hep-ex/0410041.
[16] T. Sjostrand et al., Comput. Phys. Commun. **135**, 238 (2001), hep-ph/0010017.
[17] J. S. Lee et al., Comput. Phys. Commun. **156**, 283 (2004), hep-ph/0307377.
[18] S. Eidelman et al. (Particle Data Group), Phys. Lett. **B592**, 1 (2004).
[19] M. Carena, S. Heinemeyer, C. E. M. Wagner, and G. Weiglein (1999), hep-ph/9912223.
[20] R. Eusebi, Ph.D. thesis, University of Rochester (2005).